Available online at www.sciencedirect.com
ScienceDirect
Trans. Nonferrous Met. Soc. China 19(2009) 32−39
Transactions of Nonferrous Metals Society of China
www.tnmsc.cn

Effect of Sb on microstructure of semi-solid isothermal heat-treated AZ61-0.7Si magnesium alloy

YANG Ming-bo(杨明波)[1,2], SHEN Jia(沈 佳)[1], PAN Fu-sheng(潘复生)[2]

1. College of Materials Science and Engineering, Chongqing Institute of Technology, Chongqing 400050, China;
2. College of Materials Science and Engineering, Chongqing University, Chongqing 400030, China

Received 3 January 2008; accepted 28 April 2008

Abstract: The microstructure of semi-solid isothermal heat-treated AZ61-0.7Si magnesium alloy was investigated, and compared with that of the Sb-modified AZ61-0.7Si alloy. The results indicate that it is possible to produce the AZ61-0.7Si alloy with a non-dendritic microstructure by semi-solid isothermal heat treatment, and adding 0.4% Sb can accelerate the non-dendritic microstructural evolution of the alloy. After being treated at 580 ℃ for 120 min, the Sb-modified AZ61-0.7Si alloys can obtain a non-dendritic microstructure with a higher liquid content (16%−18%) and finer unmelted primary solid particles (43−53 μm) compared with the alloy without Sb modification. In addition, after being treated at 580 ℃ for 120 min, the Mg_2Si phases in the AZ61-0.7Si alloys with and without Sb modification change from initial Chinese script shape to granule and/or polygon shapes.
Key words: magnesium alloy; AZ61-0.7Si alloy; semi-solid isothermal heat treatment; Mg_2Si phase; Sb

1 Introduction

It is well known that the semi-solid metal(SSM) processing is becoming an important forming process for the fabrication of parts for magnesium alloys. In general, the SSM processing is mainly composed of three main processes: semi-solid material production, partial remelting and thixoforming. Among those, the production of semi-solid materials with non-dendritic structure is the most important. At present, the methods of obtaining semi-solid materials include mechanical stirring(MS), electromagnetic stirring(ES), strain-induced melt activation(SIMA), spray deposition(SD), liquidus cast and semi-solid isothermal heat treatment (SSIHT)[1−2]. Among these methods, the SSIHT is a new way found in the middle 1990s. Since the SSIHT omits the special procedure to fabricate the semi-solid materials but fulfils the semi-solid non-dendritic structure during heating prior to thixoforming, the method is thought to have more development potential in the semi-solid forming for magnesium alloys. But up to now, magnesium alloys currently used in SSIHT processing are mainly restricted to a few commercial alloys such as AZ91[2]. The research about SSIHT of other magnesium alloys in the literature is very scarce.

It has been shown that the Mg-Al-Si based alloys are potential elevated temperature magnesium alloys [3−4], because the Mg_2Si phase in Mg-Al-Si based alloys has high melting point, high hardness, low density, high elastic modulus and low thermal expansion coefficient, and the Mg_2Si phase is very stable and can impede grain boundary sliding at elevated temperatures[5]. However, under the lower solidification rates the Mg-Al-Si based alloys easily form undesirable, coarse, Chinese script shaped Mg_2Si phases which would damage the mechanical properties of the alloys. Therefore, the modification and refinement of Mg_2Si phase are thought of as one of the pivotal factors to improve the mechanical properties of Mg-Al-Si based alloys. At present, the microalloying by Sb, Ca and/or P is the main method for the modification and/or refinement of Chinese script shaped Mg_2Si phases in Mg-Al-Si based alloys[6−10]. However, some research found that Sb was not an effective modifier for Mg_2Si phase[11], Ca resulted in cast defects such as a hot-crack[12], and P

Foundation item: Project(50725413) supported by the National Natural Science Foundation for Distinguished Young Scholar in China; Project (2007CB613704) by the Naitonal Basic Research Program of China; Projects(2006AA4012-9-6, 2007BB4400) supported by the Chongqing Science and Technology Commission of China
Corresponding author: YANG Ming-bo; Tel: +86-23-68667455; E-mail: yangmingbo@cqit.edu.cn
DOI: 10.1016/S1003-6326(08)60224-1

easily produced ignition and its amount was difficult to control[6]. Therefore, further research about the modification of Chinese script shaped Mg_2Si phases needs to be considered. Recent results[13] indicated that the dendritic Mg_2Si phases in Al-Si alloys might be modified to globular and/or elliptic shapes by SIHT processing. Therefore, one question arises whether the Chinese script shaped Mg_2Si phases in Mg-Al-Si based alloys can be modified by SSIHT. If the problem could be solved, not only the modification of Mg_2Si phase but also the semi-solid forming of Mg-Al-Si based alloys would be developed. But up to now, the investigation about the effect of SSIHT on the microstructure of Mg-Al-Si based alloys has not been carried out. Due to the above-mentioned reasons, the semi-solid isothermal heat-treated microstructure of AZ61-0.7Si magnesium alloy is investigated in the present work, and compared with that of the Sb-modified AZ61-0.7Si magnesium alloy.

2 Experimental

The AZ61-0.7Si alloys with and without Sb modification were prepared by melting the following materials: commercial AM60 alloy, pure Al, pure Mg, pure Zn (＞99.9%), Al-30%Si master alloy and pure Sb (＞99.9%). The experimental alloys were melted in a crucible resistance furnace and protected by a flux addition. After being treated by C_2Cl_6, the melts were held at 740 ℃ for 20 min and then poured into a permanent mould with a cavity of d 8 mm×120 mm. The actual compositions of the experimental alloys are listed in Table 1.

Table 1 Actual composition of experimental alloys (mass fraction, %)

Alloy	Al	Zn	Mn	Si	Sb	Mg
No.1 (AZ61-0.7Si)	5.92	0.79	0.24	0.68	−	Bal.
No.2 (AZ61-0.7Si-0.4Sb)	5.89	0.82	0.23	0.67	0.40	Bal.

The differential scanning calorimetry(DSC) experiment was carried out by using a NETZSCH STA 449C system in order to obtain the semi-solid isothermal heat-treated temperature of experimental alloys. Sample weighted around 30 mg was heated in a flowing argon atmosphere from room temperature to 700 ℃ for 5 min before being cooled down to 100 ℃. The heating curve was recorded at a controlling speed of 15 ℃/min. Fig.1 shows the DSC heating curves of No.1 and No.2 alloys. According to Fig.1, the onset and peak temperatures of matrix melting are 518.8 ℃ and 612.4 ℃ for No.1 alloy, 530.8 ℃ and 615.5 ℃ for No.2 alloy. In order to obtain a relatively high liquid fraction and reduce the oxidation and burning, the temperature of semi-solid isothermal heat treatment, 580 ℃, which approximately corresponded to a liquid content of 38% for No.1 alloy and 33% for No.2 alloy (the detailed calculation is given in the following section), was selected. Samples with the dimensions of 15 mm in length and 8 mm in diameter were cut from the above-mentioned alloys and put into a box-like chamber of resistance furnace. The temperature of specimen was measured with a thermocouple which was fixed on the specimen surface. The heating rate and temperature fluctuating range of the resistance furnace were 1 ℃/min and ±1 ℃, respectively. After the samples reached the experimental temperature, they were respectively held for 30, 60, 90 and 120 min, and then taken out for water quenching quickly. Fig.2 shows the schematic drawing of the sample location for the semi-solid microstructural analysis.

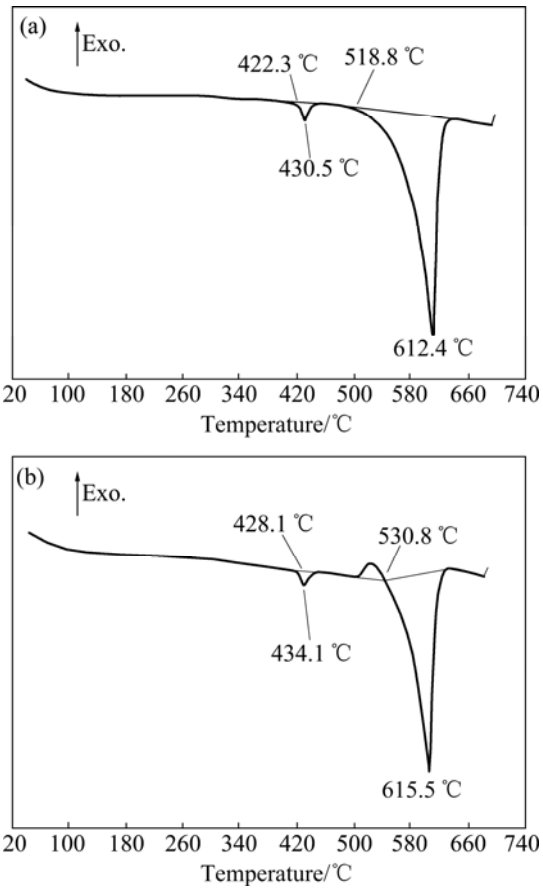

Fig.1 DSC heating curves of as-cast experimental alloys of No.1 alloy (a) and No.2 alloy (b)

After the as-cast and/or semi-solid samples were etched in an 8% nitric acid distilled water solution, the central microstructures of these samples were examined by an Olympus optical microscope and JOEL JSM-6460LV scanning electron microscope(SEM) equipped with Oxford energy dispersive X-ray spectrometer(EDS).

The grain size was analyzed by the standard linear intercept method using an Olympus stereomicroscope. The phases in the experimental alloy were also analyzed by D/Max−1200X type analyzer operated at 40 kV and 30 mA.

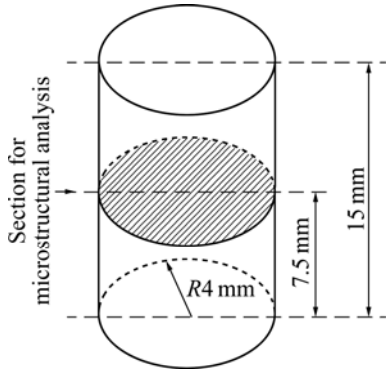

Fig.2 Schematic drawing of sample location for semi-solid microstructural analysis

3 Results and discussion

3.1 Initial as-cast microstructure

According to the XRD results, the No.1 alloy is mainly composed of α-Mg, $Mg_{17}Al_{12}$ and Mg_2Si phases, and the No.2 alloy is mainly composed of *α*-Mg, $Mg_{17}Al_{12}$, Mg_2Si and small amounts of Mg_3Sb_2 phases. Figs.3 and 4 respectively show the optical and SEM micrographs of No.1 and No.2 as-cast alloys. Similar to other Mg-Al-Si based alloys[4], the as-cast No.1 and No.2 alloys mainly consist of primary Mg-rich dendrites, eutectic mixtures and Chinese script shaped second phases (Fig.3), thereinto the eutectic mixtures fill the interdendritic region and neighboring dendrite arms interspace. According to the EDS results (Table 2), the primary Mg-rich dendrites, eutectic mixtures and Chinese script shaped second phases are *α*-Mg, $Mg_{17}Al_{12}$ and Mg_2Si phases, respectively. As expected, the dendritic *α*-Mg grains in the No.2 as-cast alloy are finer than that in the No.1 as-cast alloy (Fig.3) due to the refinement of Sb. Furthermore, it is found from Fig.4 that the Chinese script shaped morphology of Mg_2Si phases in the two alloys is very obvious, indicating that adding 0.4% Sb to AZ61-0.7Si alloy does not effectively modify the Chinese script shaped Mg_2Si phases in the alloy. Although the result is consistent with that of QUIMBY et al[11], it is contradictory to the results from YUAN et al[6].

Although the Chinese script shaped Mg_2Si phases in the No.1 and No.2 as-cast alloys are very obvious, the Mg_2Si phases in the No.2 as-cast alloy are relatively finer than those in the No.1 as-cast alloy, indicating that adding 0.4% Sb to AZ61-0.6Si alloy can refine the Chinese script shaped Mg_2Si phases in the alloy. This reason is possibly related to the enrichment of Sb at the growth interfaces of Mg_2Si phases during solidification process[7].

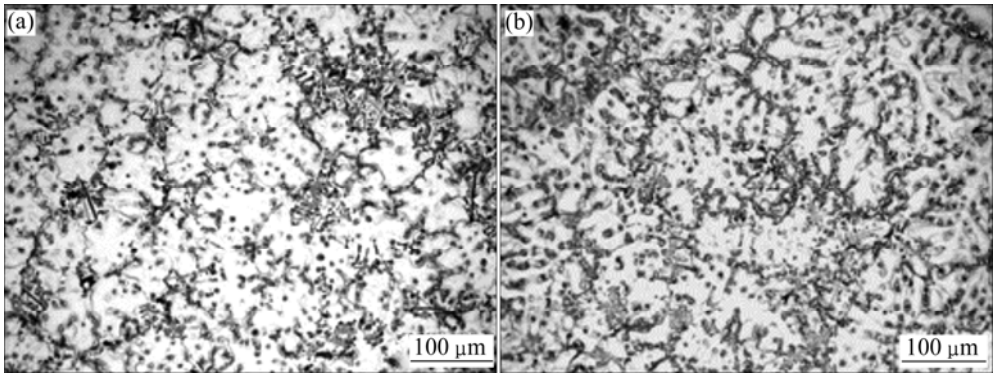

Fig.3 Optical micrographs of as-cast experimental alloys for No.1 alloy (a) and No.2 alloy (b)

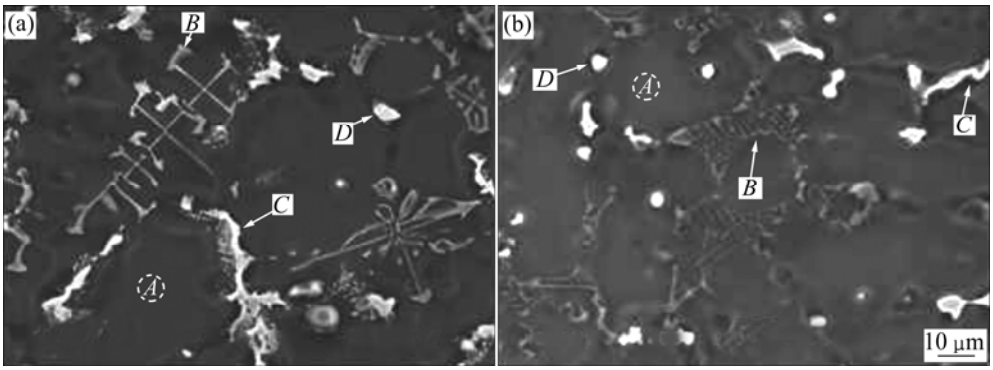

Fig.4 SEM images of as-cast experimental alloys for No.1 alloy (a) and No.2 alloy (b)

3.2 Semi-solid isothermal heat-treated microstructure

Figs.5 and 6 respectively show the microstructures of No.1 and No.2 alloys treated at 580 ℃ for different times from 30 to 120 min. It is found from Figs.5 and 6 that, when the holding time is 30 min, the liquid in No.1 and No.2 semi-solid alloys is dispersed discontinuously, and the "entrapped liquid" pool is also present inside the primary solids. With the holding time increasing from 60 to 120 min, the amount of liquid phase both inside the grains and between the grains increases, and the liquid is dispersed continuously along grain boundaries. After being treated at 580 ℃ for 120 min, the No.1 and No.2 alloys ultimately evolve into the non-dendritic microstructures with an average grain size of 53 and 43 μm for the unmelted primary solid particles, respectively. However, the unmelted primary solid particles in the No.1 semi-solid alloy are coarser and more irregular than those in the No.2 semi-solid alloy.

In general, the semi-solid microstructural evolution of an as-cast alloy experiences four stages during partial remelting [1,14]. The four stages are the initial coarsening, structural separation, spheroidization and final coarsening, respectively. However, it is found from Figs.5 and 6 that, after being treated at 580 ℃ for 120 min, the No.1 alloy appears to still remain in the structural separation stage; while the No.2 alloy appears to have entered the spheroidization stage. Then, it is concluded that adding 0.4% Sb to AZ61-0.7Si alloy can accelerate the semi-solid non-dendritic microstructural evolution of the alloy. Previous investigation [15] showed that the initial as-cast microstructures of an alloy had significant influence on its semi-solid microstructure.

Table 2 EDS results of as-cast experimental alloys (mole fraction, %)

Position	Element					Total /%
	Mg	Al	Zn	Si	Sb	
A in Fig.4(a)	94.15	4.31	1.43	0.11	−	100
B in Fig.4(a)	67.29	2.02	−	30.69	−	100
C in Fig.4(a)	64.16	32.50	1.34	−	−	100
D in Fig.4(a)	70.00	28.69	1.31	−	−	100
A in Fig.4(b)	94.92	4.66	−	0.13	0.29	100
B in Fig.4(b)	63.96	3.73	−	31.68	0.63	100
C in Fig.4(b)	64.87	33.38	1.75	−	−	100
D in Fig.4(b)	73.24	24.83	1.93	−	−	100

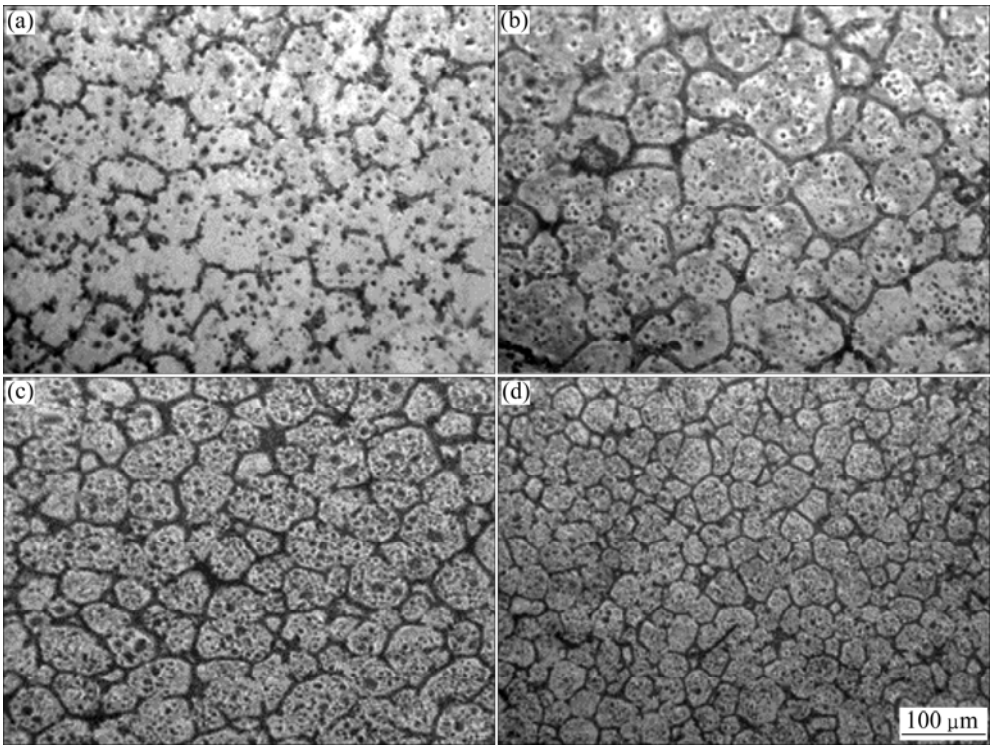

Fig.5 Microstructures of No.1 alloy treated at 580 ℃ for different time: (a) 30 min; (b) 60 min; (c) 90 min; (d) 120 min

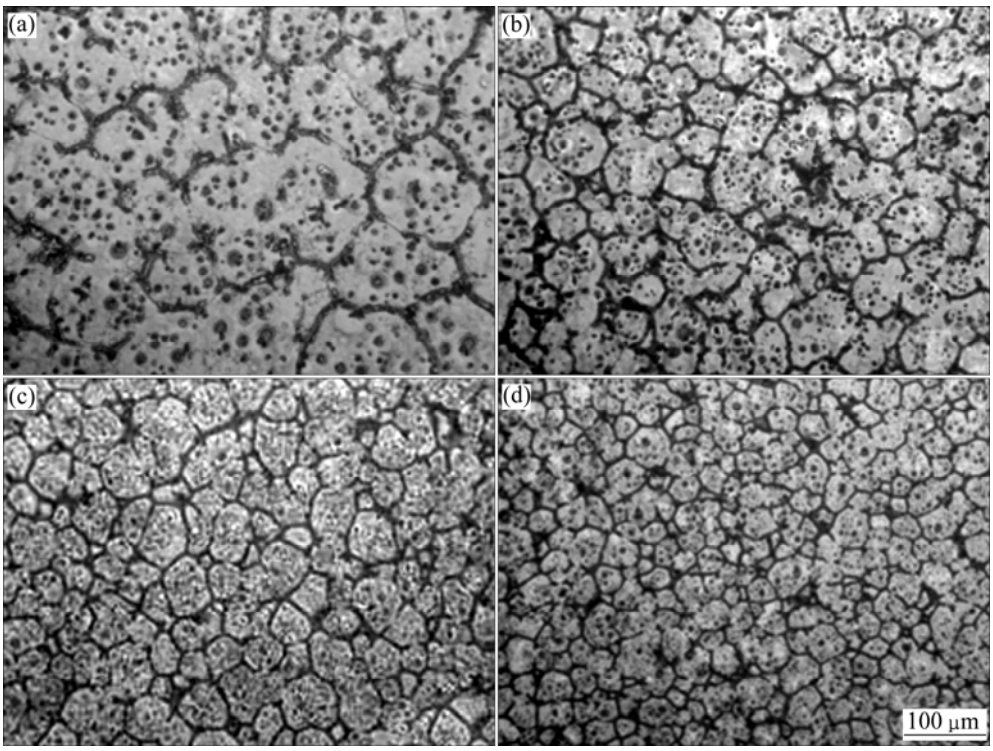

Fig.6 Microstructures of No.2 alloy treated at 580 ℃ for different time: (a) 30 min; (b) 60 min; (c) 90 min; (d) 120 min

In general, the finer the initial as-cast microstructure of an alloy is, the quicker the semi-solid microstructural evolution. Therefore, the above-mentioned results are possibly related to the refinement of initial as-cast microstructure of No.2 alloy. In addition, it is further found from Figs.5 and 6 that the final coarsening of unmelted primary solid particles in No.1 and No.2 semi-solid alloys, which is determined by the mechanisms of coalescence and Ostwald ripening[16], is not observed under the present experimental conditions. The reason is possibly related to the low volume fraction of liquid phase in No.1 and No.2 semi-solid alloys, because the low volume fraction of liquid phase retards the structural separation, spheroidization and final coarsening during semi-solid isothermal heat treatment[14]. According to the Scheil equation[17], the volume fraction of liquid, φ_L, in a semi-solid alloy should be a constant value for a given semi-solid isothermal temperature, under the assumption that the liquid homogenization is complete and no diffusion occurs in the solid.

$$\varphi_L = \left(\frac{T_M - T_L}{T_M - T}\right)^{1/(1-k)} \tag{1}$$

where T_M is the melting point of pure metal, T_L is the liquidus temperature of the alloy, T is the temperature of semi-solid isothermal heat treatment and k is the equilibrium distribution coefficient.

Under the assumption that the interactions among various alloying elements are neglected, the k of the multi-component is treated using the equivalent pseudo-binary method[18], which is expressed as

$$k = \frac{\sum m_i c_i k_i}{\sum m_i c_i} \tag{2}$$

where c_i is the initial composition of the i alloying element, m_i and k_i are the liquidus slope and partition coefficient of i element in the Mg-i binary alloys, respectively. Under the present experimental conditions, i denotes Al or Zn element. Based on the DSC results (Fig.1), the values of T_L are 612.4 ℃ and 615.5 ℃ for No.1 and No.2 alloys, respectively. The value of T_M is 650 ℃[17]. According to the Ref.[19], m_{Al}=−6.87, m_{Zn}=−6.04, k_{Al}=0.37, k_{Zn}=0.12. c_{Al} and c_{Zn} are listed in Table 1. According to Eqs.(1) and (2), the liquid fraction of No.1 and No.2 alloys at 580 ℃ respectively are 0.38 and 0.33, which are all larger than the measured liquid fractions of corresponding semi-solid alloys treated at 580 ℃ for 120 min, 0.16 and 0.18. The possible explanation is that the liquid-solid diffusion equilibrium is not reached due to short isothermal holding time in the present experiment.

In addition, the previous investigations showed that the finer the initial as-cast microstructure of an alloy is, the lower the liquid fraction of its corresponding semi-solid alloy[15]. However, as shown in Fig.7, the No.2 semi-solid alloy with finer as-cast microstructure

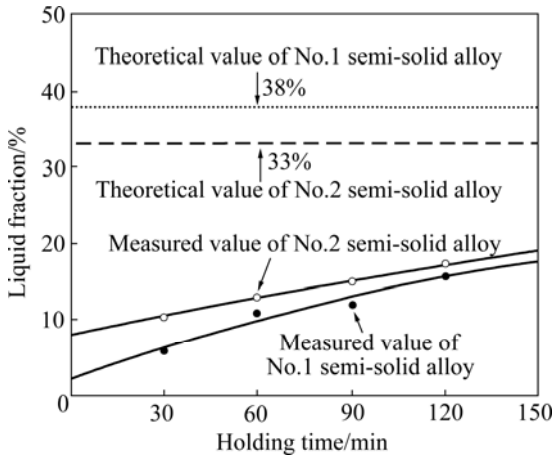

Fig.7 Effect of isothermal holding time on liquid fraction of No.1 and No.2 semi-solid alloys treated at 580 ℃

exhibits larger liquid fraction than the No.1 semi-solid alloy under the same conditions. The possible reasons are as the following: (1) the liquid-solid diffusion equilibrium does not reach due to short isothermal holding time in the present experiment; (2) the No.1 alloy contains more eutectic phases whose dissolving and diffusing need longer time to reach an equilibrium state. However, it is estimated that, if a longer holding time is adopted, the liquid fraction in the No.1 semi-solid alloy would ultimately exceed that in the No.2 semi-solid alloy due to the higher volume fraction of eutectic phases in the No.1 alloy.

Considering that 40%−60% liquid content is generally defined as a working range of SSM in order to obtain adequate flow ability for a semi-solid slurry[16], in further study, a longer isothermal holding time than 120 min and a higher semi-solid isothermal treated-temperature than 580 ℃ should be considered for the AZ61-0.7Si alloy.

3.3 Modification analysis of Mg_2Si phase

Fig.8 and Table 3 respectively show the SEM images and the EDS results of No.1 and No.2 semi-solid alloys treated at 580 ℃ for 120 min. It is found from Fig.8 that the fine secondary α-Mg phases are surrounded by $Mg_{17}Al_{12}$ phases. In addition, it is proved from Tables 2 and 3 that little Si dissolves in the matrix after semi-solid isothermal heat treatment and Si is still in the form of Mg_2Si in the alloys. However, it is interestingly found from Fig.8 that, after being treated at 580 ℃ for 120 min, the Mg_2Si phases in the No.1 and No.2 alloys change from initial Chinese script shape to granule and/or polygon shapes, indicating that the semi-solid isothermal heat treatment can modify the Chinese script shaped Mg_2Si phases in the AZ61-0.7Si alloy.

Since the melting temperature of Mg_2Si phase is

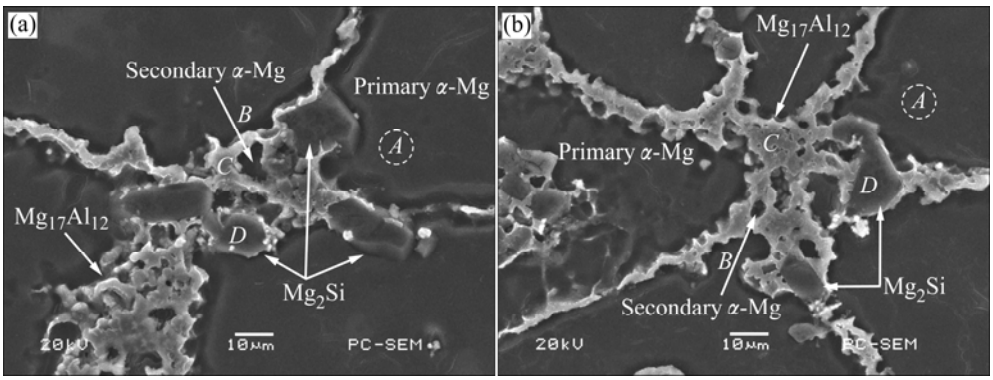

Fig.8 SEM images of precipitates between grains of secondary microstructures for different semi-solid alloys: (a) No.1 alloy; (b) No.2 alloy

Table 3 EDS results of semi-solid experimental alloy (mole fraction, %)

Position	Element					Total/%
	Mg	Al	Zn	Si	Sb	
A in Fig.8(a)	93.00	5.14	1.74	0.12	−	100
B in Fig.8(a)	91.66	6.21	2.13	−	-	100
C in Fig.8(a)	67.14	30.04	2.73	0.09	−	100
D in Fig.8(a)	60.11	0.63	−	39.26	−	100
A in Fig.8(b)	94.22	5.33	−	0.15	0.30	100
B in Fig.8(b)	92.03	5.76	2.21	−	−	100
C in Fig.8(b)	63.04	32.85	3.92	0.11	0.08	100
D in Fig.8(b)	61.98	0.67	−	36.7	0.65	100

1 085 ℃[16], the modification of Chinese script shaped Mg_2Si phase during the semi-solid isothermal heat treatment can not be achieved by melting mode. It is well known that the temperature and solute concentration fluctuate during the solidification process. Therefore, on the surface of Mg_2Si phase curvature fluctuation should occur. Based on the above analysis, one possible explanation for the modification of Chinese script shaped Mg_2Si phases during semi-solid isothermal heat treatment, can be obtained by using the Gibbs-Thomson effect[20]. According to the Gibbs-Thomson formula, the Si concentration in the matrix corresponding to the site where the Mg_2Si phase has larger curvature, can be expressed as[20]

$$c_\alpha(r) = c_\alpha(\infty)\exp\left(\frac{2\sigma V_B}{k_B T r}\right) \tag{3}$$

where $c_\alpha(r)$ is the Si concentration at the position with a curvature radius r, $c_\alpha(\infty)$ is the Si concentration at flat interface, σ is the surface tension, V_B is the volume of Si atom, T is the temperature and k_B is the coefficient related to the shape.

According to Eq.(3), the smaller the curvature radius is, the higher the Si concentration. Since the curvature radius at different positions for a Chinese script shaped Mg_2Si particle might be different, a gradient of Si concentration could exist between these positions. Therefore, during the semi-solid isothermal heat treatment, the Si atoms would diffuse from the position where the curvature and Si concentration are respectively large and high to the flat interface where the Si concentration is lower, and then the balance of local Si concentration between these positions would be broken. Furthermore, in order to keep the balance of Si concentration, these positions with larger curvature would be dissolved. Oppositely, due to the supersaturation of Si concentration, the Mg_2Si phases would form in the α-Mg matrix corresponding to the flat interface. As a result, these positions with larger curvature would break, and then the granule and/or polygon shaped Mg_2Si phase, would form. The process can be illustrated in Fig.9. As shown in Fig.9, the curvatures of these positions such as '*A*' and '*B*' in Fig.9(a) are larger, so these positions would be firstly dissolved (Fig.9(b)). With the gradual diffusion of Si atoms, the Mg_2Si particle would break up in these positions such as '*A*' and '*B*', as shown in Figs.9(c) and (d). Finally, with the prolonging of the semi-solid isothermal holding time, the granule and/or polygon shaped Mg_2Si particles which have close curvature radius at different positions would form (Figs.9(d) and (e)).

In spite of the above studies, the modification mechanism of Chinese script shaped Mg_2Si phases during semi-solid isothermal heat treatment, is not completely clear, and further investigation needs to be carried out. For example, the majority of $Mg_{17}Al_{12}$ and Mg_2Si phases in the as-cast experimental alloy connects with each other (Fig.4), and the Mg_2Si phases in the semi-solid alloys tightly contact with the partially remelted liquid at the grain boundaries (Fig.8). Therefore, one question whether the modification of Chinese script shaped Mg_2Si phases during semi-solid isothermal heat treatment is effected by the penetration of remelted liquid and the diffusion of Al atoms in the remelted liquid, still remains. The question is a subject for further study in our group.

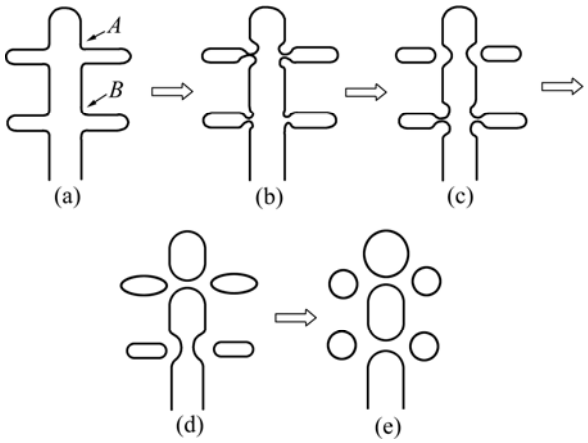

Fig.9 Sketch of dissolving and breaking process of Chinese script shaped Mg_2Si phase in larger curvature site: (a) Mg_2Si phase; (b) Dissolving; (c) Breaking+dissolving; (d) Granulating +breaking; (e) Granulating

4 Conclusions

1) It is possible to produce the AZ61-0.7Si alloy with a non-dendritic microstructure by the semi-solid isothermal heat treatment, and adding 0.4% Sb to AZ61-0.7Si alloy can accelerate the non-dendritic microstructural evolution of the alloy. After being treated at 580 ℃ for 120 min, the Sb-modified AZ61-0.7Si alloys can obtain a non-dendritic microstructure with a higher liquid content (18%−16%) and finer unmelted primary solid particles (43−53 μm) than the alloy without Sb modification.

2）The Chinese script shaped Mg_2Si phases in the AZ61-0.7Si alloy may be modified by semi-solid isothermal heat treatment. After being treated at 580 ℃ for 120 min, the Mg_2Si phases in the AZ61-0.7Si alloys with and without Sb modification change from the initial Chinese script shape to granule and/or polygon shapes.

References

[1] CHEN T J, MA Y, HAO Y, LU S, XU G J, SUN J. Structural

evolution of ZA27 alloy during semi-solid isothermal heat treatment [J]. Trans Nonferrous Met Soc China, 2001, 11(1): 98−102.

[2] KIM J M, KIM K T, JUNG W J. Effects of isothermal heating procedure and strontium addition on semisolid forming of AZ91 magnesium alloy [J]. Mater Sci Technol, 2002, 18: 698−701.

[3] YANG M B, PAN F S, ZHANG J, ZHANG J. An analysis of the development and applications of current and new Mg-Al based elevated temperature alloys [J]. Mater Sci Forum, 2005, 488/489: 923−926.

[4] DARGUSCH M S, BOWLES A L, PETTERSEN K, BAKKE P, DUNLOP G L. The effect of silicon content on the microstructure and creep behavior in die-cast magnesium AS alloys [J]. Metal Mater Trans A, 2004, 35: 1905−1909.

[5] EVANGELISTA E, GARIBOLDI E, LOHNE O, SPIGARELLI S. High-temperature behaviour of as die-cast and heat treated Mg-Al-Si AS21X magnesium alloy [J]. Mater Sci Eng A, 2004, 387/389: 41−45.

[6] YUAN G Y, LIU Z L, WANG Q D, DING W J. Microstructure refinement of Mg-Al-Zn-Si alloys [J]. Mater Lett, 2002, 56: 53−58.

[7] SRINIVASAN A, PILLAI U T S, PAI B C. Microstructure and mechanical properties of Si and Sb added AZ91 magnesium alloy [J]. Metal Mater Trans A, 2005, 36: 2235−2243.

[8] NAM K Y, SONG D H, LEE C W, LEE S W, PARK Y H, CHO K M, PARK I M. Modification of Mg_2Si morphology in as-cast Mg-Al-Si alloys with strontium and antimony [J]. Mater Sci Forum, 2006, 510/511: 238−241.

[9] KIM J J, KIM D H, SHIN K S, KIM N J. Modification of Mg_2Si morphology in squeeze cast Mg-Al-Zn-Si alloys by Ca or P addition [J]. Scripta Mater, 1999, 41: 333−340.

[10] YOO M S, SHIN K S, KIM N J. Effect of Mg_2Si particles on the elevated temperature tensile properties of squeeze-cast Mg-Al alloys [J]. Metal Mater Trans A, 2004, 35: 1629−1632.

[11] QUIMBY P D, LU S Z, PLICHTA R, VISSER D K, JACOBE K P. Effects of minor addition and cooling rate on the microstructure of cast magnesium-silicon alloys [C]// LUO A, NEELAMEGGHAM N, BEALS R. Magnesium Technology. San Antonio, Texas, USA: TMS, 2006: 535−538.

[12] TANG B, LI S S, WANG X S, ZENG D B, WU R. An investigation on hot-crack mechanism of Ca addition into AZ91D alloy [J]. J Mater Sci, 2005, 40: 2931−2936.

[13] QIN Q D, ZHAO Y G, XIU K, ZhOU W, LIANG Y H. Microstructure evolution of in situ Mg_2Si/Al-Si-Cu composite in semisolid remelting processing [J]. Mater Sci Eng A, 2005, 407: 196−200.

[14] WANG J L, SU Y H, TSAO C Y A. Structural evolution of conventional cast dendritic and spray-cast nonodendritic structures during isothermal holding in the semi-solid state [J]. Scripta Mater, 1997, 37: 2003−2007.

[15] CHEN T J, HAO Y, SUN J, LI Y D. Effects of Mg and RE additions on the semi-solid microstructure of a zinc alloy ZA27 [J]. Sci Technol Adv Mater, 2003, 4: 495−502.

[16] CZERWINSKI F. The processing phenomena of semisolid Mg-9Al-1Zn alloy at ultra high contents of the unmelted phase [J]. Mater Sci Eng A, 2005, 392: 51−61.

[17] ZHANG Q Q, CAO Z Y, ZHANG Y F, SU G H, LIU Y B. Effect of compression ratio on the microstructure evolution of semisolid AZ91D alloy [J]. J Mater Proc Technol, 2007, 184: 195−200.

[18] LI D Z, HU Z Y, LI Q, LI Y Y. Microstructure simulation and process optimization of turbine blade castings [J]. Acta Metallurgica Sinica (English Letters), 1998, 11: 383−390.

[19] ZENG X Q, WANG Y X, DING W J, LUO A A, SACHDEV A K. Effect of strontium on the microstructure, mechanical properties, and fracture behavior of AZ31 magnesium alloys [J]. Metal Mater Trans A, 2006, 37: 1333−1341.

[20] NISHIOKA K, MAKSIMOV I L. Reconsideration of the concept of critical nucleus and the Gibbs-Thomson equation [J]. J Crystal Growth, 1996, 163: 1−7.

(Edited by YUAN Sai-qian)